Hindawi
Journal of Nanomaterials
Volume 2019, Article ID 7936143, 13 pages
https://doi.org/10.1155/2019/7936143

Research Article

Characterization and Evaluation of HGF-Loaded PLGA Nanoparticles in a CCl_4-Induced Acute Liver Injury Mouse Model

Chuxi Lin,[1,2] Xueer Wang,[2] Nuyun Liu,[3] Qing Peng,[1] Yang Li,[1] Lin Zhang ,[2] and Yi Gao [1,4]

[1]*Department of Hepatobiliary Surgery II, Guangdong Provincial Research Center for Artificial Organ and Tissue Engineering, Guangzhou Clinical Research and Transformation Center for Artificial Liver, Institute of Regenerative Medicine, Zhujiang Hospital, Southern Medical University, Guangzhou, Guangdong Province, China*
[2]*Department of Histology and Embryology, Guangdong Provincial Key Laboratory of Tissue Construction and Detection, School of Basic Medical Sciences, Southern Medical University, Guangzhou, China*
[3]*Institute of Comparative Medicine & Laboratory Animal Center, Southern Medical University, Guangzhou 510515, China*
[4]*State Key Laboratory of Organ Failure Research, Southern Medical University, Guangzhou, China*

Correspondence should be addressed to Lin Zhang; zlilyzh@126.com and Yi Gao; drgaoy@126.com

Received 3 May 2019; Accepted 19 June 2019; Published 7 October 2019

Academic Editor: Peter Reiss

Liver injury can be caused by various harmful factors since the liver is considered the key organ for detoxifying endogenous and exogenous substances. Hepatocyte growth factor (HGF) can regulate redox homeostasis through the expression of antioxidant proteins when the liver is under injury. However, HGF is easily degraded. In this study, we produced three kinds of HGF-loaded poly(lactic-co-glycolic) acid (PLGA) nanoparticles with an initial addition of 2 μg HGF (NPs-HGF-2 μg), 4 μg HGF (NPs-HGF-4 μg), and drug-free nanoparticles (NPs) using the W/O/W emulsion-solvent evaporation method in accordance with our patent. The morphology and physical characteristics were analyzed, and effects of HGF-loaded PLGA nanoparticles on a CCl_4-induced acute liver injury mouse model were investigated and compared with HGF solutions. We observed that the morphology and the physical characteristics of the nanoparticles were almost the same, with similar sizes, polydispersity, and zeta potential. HGF-loaded PLGA nanoparticles maintained higher HGF concentrations for a longer period of time in blood and liver tissues. HGF-loaded PLGA nanoparticles increased the SOD activity and GPX levels, decreased the MDA levels in the liver, reduced the necrotic areas of the liver, and decreased the levels of AST, ALT, ALP, T-BIL, BUN, and Scr in blood. In conclusion, our technique for preparing HGF-loaded PLGA nanoparticles was stable and the products were of good quality. HGF-loaded PLGA nanoparticles could provide greater therapeutic benefits on CCl_4-induced acute liver injury, including antilipid peroxidation and a reduction in indicator enzymes of liver injury.

1. Introduction

Liver injury is caused by various harmful factors since the liver is considered the key organ for detoxifying endogenous and exogenous substances [1]. It could be induced by viruses, drugs, alcohol, and parasites [2]. The incidence of acute liver injury is increasing because of drug abuse or overdoses of some medications [3, 4]. Oxidative stress is a major cause of acute liver injury [5]. The CCl_4-induced acute liver injury mouse model is well established and is widely used in scientific research. A single dose of CCl_4 can cause the release of free radicals, which can lead to oxidative stress-induced liver diseases and acute necrosis of the liver [6, 7].

Hepatocyte growth factor (HGF) is a liver cell mitogen that plays an important role in liver regeneration and repair after injury [8, 9]. HGF acts as an antihepatitis agent when the liver is under injury [10]. It can regulate redox homeostasis through the expression of antioxidant proteins [11, 12], such as superoxide dismutase (SOD) and glutathione peroxidase (GPX). However, HGF has poor stability in vitro and is easily degraded by enzymes in vivo [13].

To improve the stability and bioavailability of HGF, our laboratory recently explored an optimal condition for

preparing HGF-loaded poly(lactic-co-glycolic) acid (PLGA) nanoparticles and evaluated its bioactivities [14]. However, the biological activity of HGF-loaded PLGA nanoparticles has been verified only at the cellular level. In the present study, we prepared three kinds of PLGA nanoparticles with different initial additions of HGF. The morphologies and physical characteristics were analyzed, and the effects of HGF-loaded PLGA nanoparticles on a CCl_4-induced acute liver injury mouse model were further investigated.

2. Materials and Methods

2.1. Cell Culture. Human hepatoma cells (HepG2) were purchased from ATCC (ATCC HB-8065). HepG2 cells were maintained in Dulbecco's modified Eagle's medium (DMEM, Thermo Fisher Scientific Inc., USA) containing 10% fetal bovine serum and 1% penicillin/streptomycin solution (P/S) at 37°C in 5% CO_2.

2.2. CCK-8 Assay. HepG2 proliferation was assessed using a Cell Counting Kit-8 assay (CCK-8 assay; Bimake, USA) according to the manufacturer's instructions. A concentration of 3×10^3 cells was seeded into 96-well culture plates in 100 μl complete growth medium. The cells were then serum-starved for 24 h. HGF was added at various concentrations (1, 10, 20, 40, 80, 160, 320, 640, and 1280 ng/ml), and 5 wells were investigated for each concentration. After treatment with HGF for 24, 48, 72, 96, and 120 h, a 10 μl/well Cell Counting Kit-8 (CCK-8) reagent was added and the cells were incubated for 2 h at 37°C until the color changed to orange. The results were acquired by measuring the absorbance at a wavelength of 450 nm using an ELx800 microplate reader (BioTek Instruments Inc., USA).

2.3. Preparation of HGF-Loaded PLGA Nanoparticles. Empty nanoparticles were prepared by the double emulsion-solvent evaporation method, as reported in our previous study. Twenty-five milligrams of poly(lactide-co-glycolide) (PLGA, 50 : 50, 24-38 kDa, Thermo Fisher Scientific Inc.) was dissolved in 750 μl dichloromethane and 250 μl acetone (both from Guangzhou Chemical Reagent Factory, Guangzhou, China) as the oil phase (O). Five milligrams of bovine serum albumin (BSA, GBCBIO Technologies Inc., Guangzhou, China) with 10 mg of mannitol, 5 mg of sucrose, and 5 μl of polyethylene glycol 400 (PEG-400) (all from Guangzhou Chemical Reagent Factory, Guangzhou, China) was dissolved in 100 μl of water as the water phase (W1). The first emulsion (W1/O) was obtained using an Omni Ruptor 4000 ultrasonic homogenizer (OMNI International, USA) at 70% power for one minute with a 10% pulse. Then, the first emulsion was added into 3 ml of 1% (w/v) poly(vinyl alcohol) (PVA, 13-23 kDa, Thermo Fisher Scientific Inc., USA) (W2) and sonicated with the previously mentioned parameters to generate the W1/O/W2 emulsion. Later, the emulsion was added dropwise to 40 ml of 0.3% (w/v) PVA and stirred at 800 rpm for 4 h at ambient temperature. The nanoparticle suspension was then washed twice in sterile water by centrifugation (Optima XPN-100 ultracentrifuge, Beckman Coulter, USA) for 20 min at 14000 rpm and 4°C. The preparation of HFG-loaded nanoparticles was made following the same procedure as the nonloaded particles (NPs) with a dose of 2 μg and 4 μg HGF (recombinant mouse HGF, R&D Systems) added into the water phase, respectively. All nanoparticles were then freeze-dried and lyophilized (Epsilon 1-4 LSCplus, Christ, Germany) for 24 h and stored at 4°C for further use.

2.4. Characterization of the Nanoparticles

2.4.1. Nanoparticle Morphology. The surface and internal morphology of the nanoparticles were examined using transmission electron microscopy (TEM) (H-7650, Hitachi, Japan). One drop of nanoparticle suspension was placed directly onto a TEM sample holder coated with 3% phosphotungstic acid solution for 2 min and air-dried for 30 min before the analysis.

2.4.2. Nanoparticle Size, Polydispersity, and Zeta Potential. Nanoparticle size, polydispersity, and zeta potential were analyzed by a zeta potential analyzer (Zetasizer Nano ZS, Malvern, UK). Approximately 1 ml of nanoparticle suspension was added to the test cells.

2.4.3. The Release Kinetics of the Nanoparticles. A certain amount of nanoparticles were weighed and placed in the dialysis membrane (Spectrum, USA) and were added into small glass vials with 5 ml physiological saline. The glass vials were put into a constant temperature shaker with a temperature of 37°C and a speed of 72 rpm. At 4, 8, 12, 24, 48, 72, 96, 120, and 168 h, 500 μl solution was taken out and 500 μl fresh physiological saline was replenished into the glass vials. Concentrations of HGF were determined by a HGF ELISA kit (Bioswamp, Wuhan, China), and concentrations of BSA were measured by a BCA kit (Beyotime Biotechnology, Shanghai, China) following the manufacturer's instructions.

2.4.4. The Drug Loading of the Nanoparticles. About 10 mg nanoparticles were weighted and dissolved in 500 μl dichloromethane. Then, 500 μl distilled water was added to extract HGF or BSA from the nanoparticles. Extraction liquid was collected for 3 times. Concentrations of HGF were determined by a HGF ELISA kit, and concentrations of BSA were measured by a BCA kit following the manufacturer's instructions:

$$\text{Drug loading} = \frac{\text{protein contented in nanoparticles}}{\text{total amount of nanoparticles}} = \text{concentrations of HGF or BSA (mg/ml)} * \frac{1.5\,\text{ml}}{10\,\text{mg}} * 100\% \quad (\text{unit : mg BSA or HGF/mg nanoparticle} * 100\%). \tag{1}$$

2.4.5. The Loading Efficiency of the Nanoparticles.

$$\text{Loading efficiency} = \frac{\text{protein contented in nanoparticles}}{\text{initial dose of protein}} = \text{total amount of nanoparticles} * \frac{\text{drug loading}}{\text{initial dose of protein}} * 100\%. \quad (2)$$

2.5. Animal Experiments. Forty-two male C57BL/6 mice aged 6 to 8 weeks and weighing 18-24 g were obtained from the Southern Medical University Laboratory Animal Center. The mice were maintained in individual cages on a 12-hour light and 12-hour dark photoperiod and fed with standard rodent chow and water. All animal experiments were performed according to the National Institutes of Health *Guide for the Care and Use of Laboratory Animals* and were approved by the Institutional Animal Care and Use Committee (IACUC) at Southern Medical University.

The mice were randomly separated into seven groups (6 mice/group). Group 1 was a negative control group (normal). The remaining 6 groups received normal saline (untreated), empty nanoparticles (NPs), two doses of HGF solution, and two doses of HGF nanoparticles three days before they received a single intraperitoneal injection of 10 ml/kg body weight of 30% CCl_4 (carbon tetrachloride, Shanghai Macklin Biochemical Co. Ltd., Shanghai, China) suspended in olive oil (Shanghai Macklin Biochemical Co. Ltd., Shanghai, China). Since the circulating blood volume accounts for 6% of the body weight of a mouse, a mouse weighing 18-24 g may have an average blood volume of 1.5 ml [15]. The HGF solution groups were injected with a dose of 60 ng HGF and 120 ng HGF through the tail vein to ensure that the mice were administered a blood concentration of 40 ng HGF per milliliter of blood (40 ng/ml HGF) and 80 ng HGF per milliliter of blood (80 ng/ml HGF), respectively. The HGF nanoparticle groups (HGF-NPs-2 μg and HGF-NPs-4 μg groups) were then administered approximately 10 mg of HGF nanoparticles with different doses of HGF that were prepared with our preparation process. The two doses of HGF nanoparticles could release a total dose of 60 ng and 120 ng HGF, respectively, until the mice were sacrificed according to our previous study. Mice were sacrificed 24 h after acute liver failure was induced. Body weight and liver weight were analyzed. Liver tissues and blood samples were collected for subsequent assays.

2.6. Analysis of Biochemical Indicators. HGF levels in the blood and in the liver tissues were analyzed using a HGF ELISA kit.

Serum alanine aminotransferase (ALT), aspartate aminotransferase (AST), total bilirubin (T-BIL), and alkaline phosphatase (ALP) levels were determined using the ALT, AST, T-BIL, and ALP reagent kits (Changchun Huili Biotech Co. Ltd., Jilin, China) according to the manufacturer's instructions. Blood urea nitrogen (BUN) and serum creatinine (Scr) levels were analyzed using the BUN and Scr reagent kits (Changchun Huili Biotech Co. Ltd., Jilin, China). Superoxide dismutase (SOD), glutathione peroxidase (GPX), and malondialdehyde (MDA) were analyzed using the SOD, GPX, and MDA standard diagnostic kits (Nanjing Jiancheng Bioengineering Institute, Nanjing, China) according to the manufacturer's protocols.

2.7. Histological Examination. Liver tissue samples were fixed in 4% paraformaldehyde and embedded in paraffin after dehydration with a graded series of ethanol. The tissues were sectioned at 5 mm, and hematoxylin and eosin (H&E) staining was performed according to the standard procedures. All sample sections were observed under a microscope (Leica, Germany). The diseased regions of each section were labeled by a pathologist who was not related to our study from the Department of Pathology of Southern Medical University, China. The areas of diseased regions were analyzed using ImageJ software.

2.8. Statistical Analysis. Statistical analysis was performed using GraphPad Prism 7 software. Data are presented as the mean ± standard error. One-way ANOVA were assessed for comparisons between groups. A P value of 0.05 was considered statistically significant.

3. Results

3.1. HGF Induced HepG2 Cell Proliferation in a Dose-Dependent Manner. Cultured HepG2 cells were used to investigate the effects of HGF on cell proliferation, and HepG2 proliferation was assessed using a Cell Counting Kit-8 (CCK-8) assay. The CCK-8 assay results showed that HGF significantly promoted HepG2 cell proliferation at the doses of 40 and 80 ng/ml during the five-day incubation with different concentrations of HGF (0, 1, 10, 20, 40, 80, 160, 320, 640, and 1280 ng/ml HGF) (Figure 1(b)). The two doses were used in the following experiments.

3.2. Formulations and Physical Characteristics of HGF-Loaded PLGA Nanoparticles and PLGA Nanoparticles. Three kinds of nanoparticles were prepared using the double (W1/O/W2) emulsion-solvent evaporation method with PVA as the stabilizer in accordance with our patent as follows: drug-free nanoparticles (NPs), nanoparticles with an initial addition of 2 μg HGF (HGF-NPs-2 μg), and nanoparticles with an initial addition of 4 μg HGF (HGF-NPs-4 μg).

The morphologies of nanoparticles are shown in Figures 2(a)–2(c). The nanoparticles showed a similar size and zeta potential with a polydispersity about 0.2 (Table 1), indicating that the nanoparticles were stable. The nanoparticles of both concentrations of HGF were successfully prepared in terms of morphology, and the physical characteristics of the nanoparticles were the same as those reported in our previous study [14]. Drug loading of the HGF-loaded nanoparticles was about $0.001268 \pm 0.000058\%$ and $0.002422 \pm 0.000030\%$ (unit: mg HGF/mg nanoparticle $*$ 100%), respectively (Table 1). The release curves of the three kinds of nanoparticles were shown in Figure 2(d). The release performance of the three nanoparticles could be summarized as follows: the initial burst release stage, the slow release stage, and the gradual plateau stage.

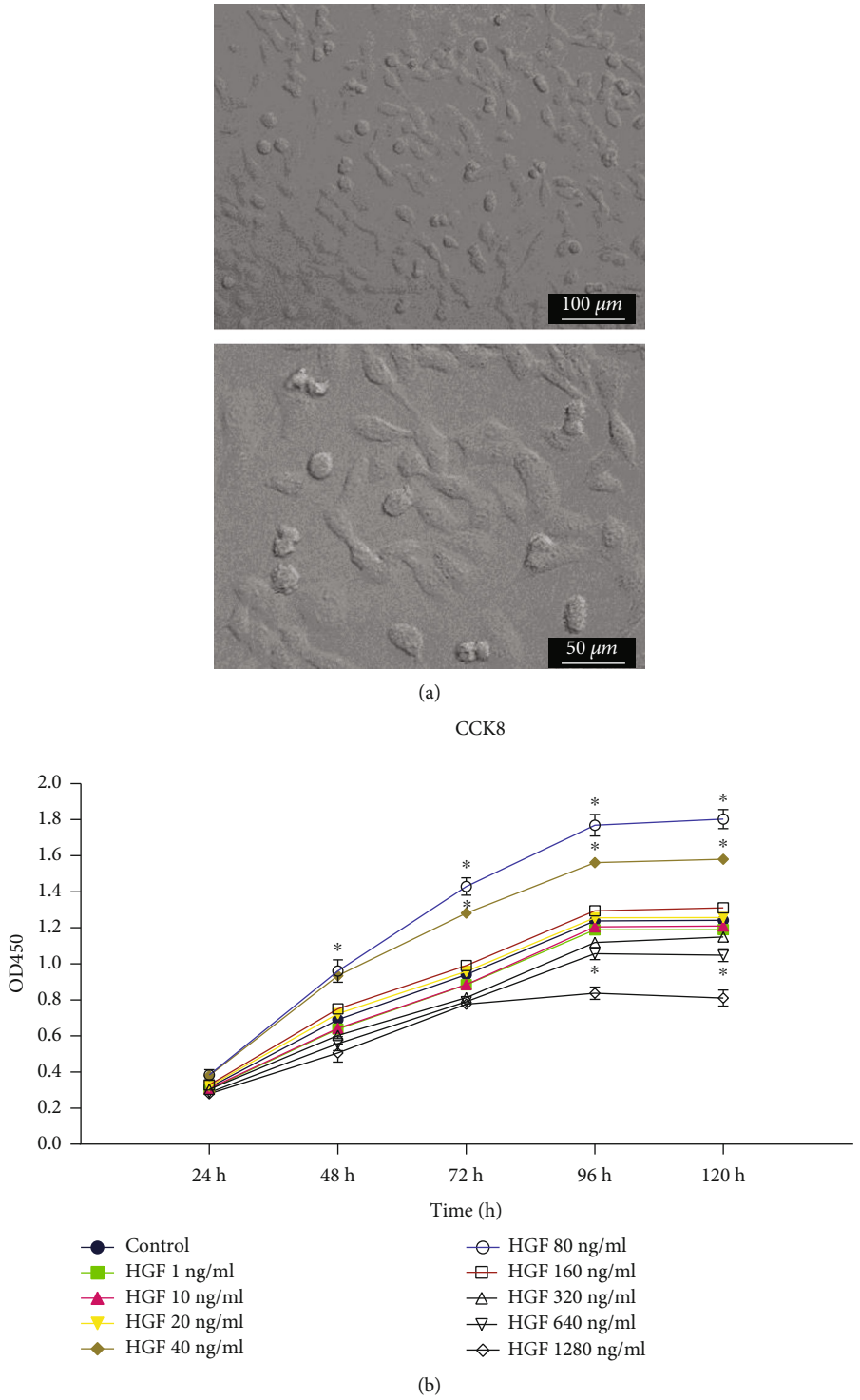

Figure 1: HGF induced HepG2 cell proliferation in a dose-dependent manner. (a) Optical microscope imaging (×10 and ×20) of the morphology of HepG2 cells; after 24 h, they were seeded into a 96-well plate. (b) The CCK-8 assay showed that HGF significantly promoted HepG2 proliferation at concentrations of 40 and 80 ng/ml. Data are shown as the mean ± SD. $^*P < 0.05$ versus the control group.

At 72 h, the cumulative release percentages of HGF-NPs-2 μg and HGF-NPs-4 μg were $55.3 \pm 0.8\%$ and $52.8 \pm 0.3\%$, respectively. Approximately 60 ng HGF and 120 ng HGF could be released from 10 mg of the two kinds of HGF-loaded PLGA nanoparticles at 72 h.

3.3. HGF-Loaded PLGA Nanoparticles Maintained Higher HGF Concentrations for a Longer Period of Time in the Blood and Liver Tissues. Since the circulating blood volume accounts for 6% of the body weight of a mouse, a mouse weighing 18-24 g may have an average blood volume of

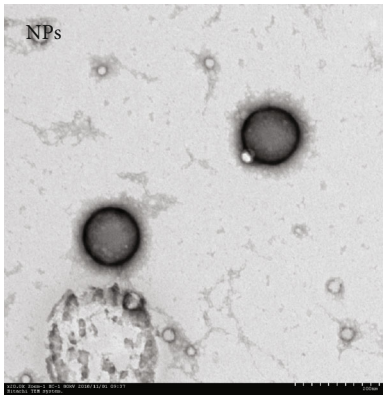

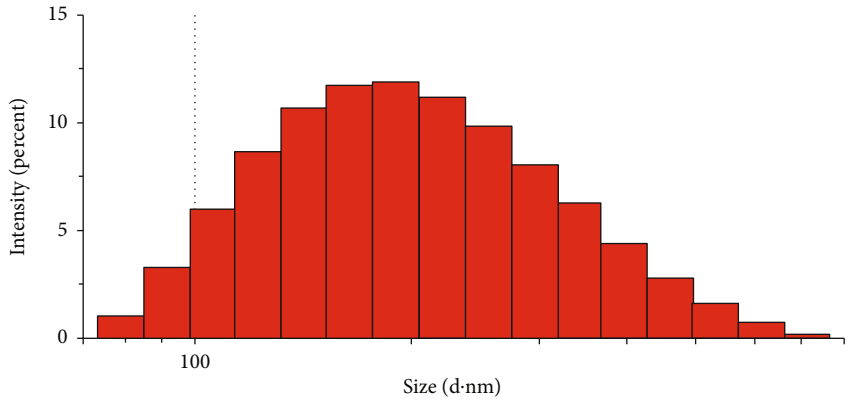

(a)

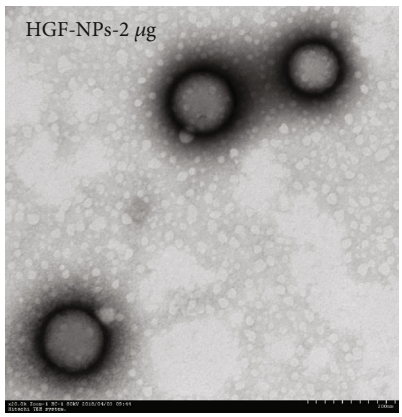

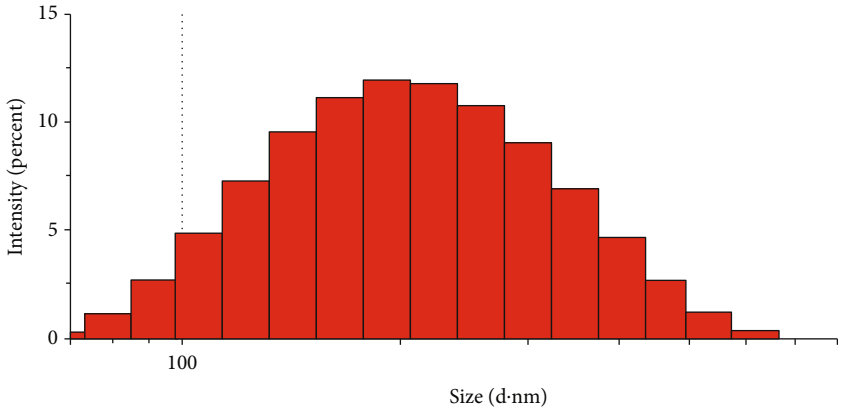

(b)

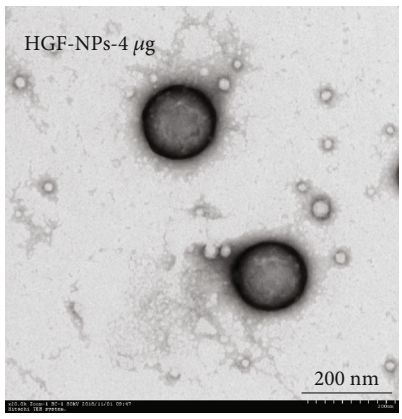

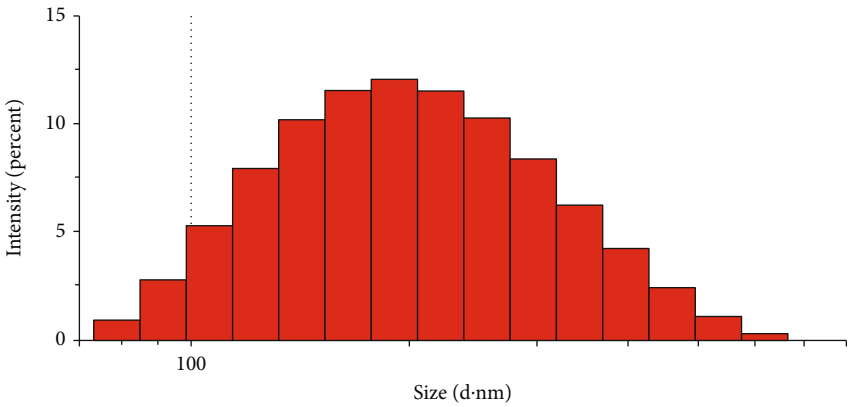

(c)

Figure 2: Continued.

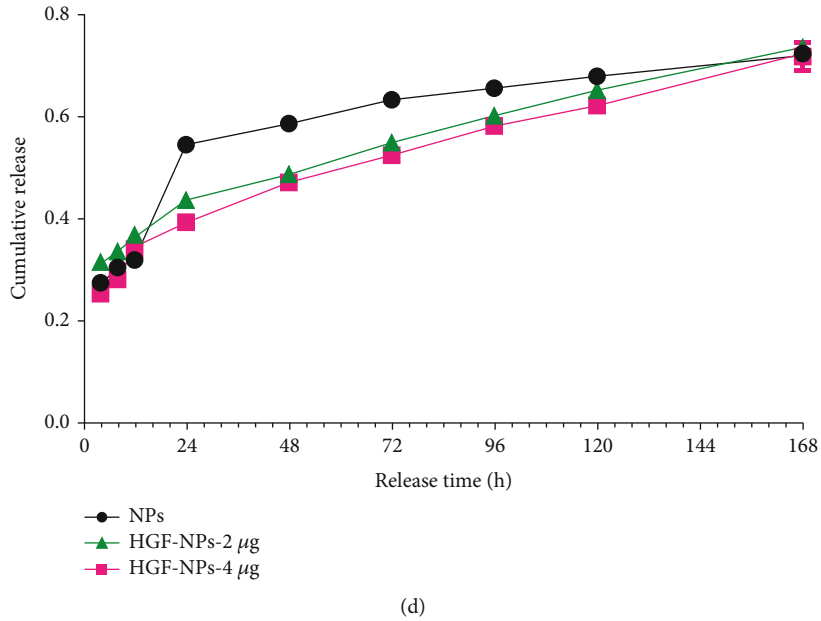

(d)

Figure 2: The morphology and physical characteristics of HGF-loaded PLGA nanoparticles. (a–c) Transmission electron microscopy images of HGF-loaded PLGA nanoparticles (NPs, HGF-2 μg-NPs, and HGF-4 μg-NPs) and their corresponding histograms of size data provided by DLS. (d) The release curves of the three kinds of nanoparticles.

Table 1: Properties of the nanoparticles (mean ± SD, $n = 3$).

	NPs	HGF-NPs-2 μg	HGF-NPs-4 μg
Size by intensity (nm)	187.50 ± 3.15	193.03 ± 3.39	193.23 ± 4.24
Polydispersity	0.194 ± 0.012	0.228 ± 0.004	0.251 ± 0.014
Zeta potential (mV)	-43.13 ± 1.27	-47.47 ± 0.31	-47.23 ± 0.57
Drug loading (%)	4.13 ± 0.44*	0.001268±0.000095**	0.002422±0.000052**
Loading efficiency (%)	15.27 ± 1.22	11.78 ± 1.34	11.79 ± 0.35

The 3 measurements of the samples come from 3 different samples, which showed that our procedure and nanoparticle quality are stable. Size by intensity, polydispersity, and zeta potential are measured by a zeta potential analyzer. Drug loading is calculated by drug loading = protein contented in nanoparticles/total amount of nanoparticles (unit : *mg BSA/mg nanoparticle ∗ 100%; **mg HGF/mg nanoparticle ∗ 100%). Loading efficiency is calculated by loading efficiency = total amount of nanoparticles ∗ drug loading/initial dose of protein ∗ 100%.

1.5 ml [15]. From the previous results, we found that 40 and 80 ng/ml HGF could significantly promote HepG2 cell proliferation and 60 ng HGF and 120 ng HGF could be released from 10 mg of the two kinds of HGF-loaded PLGA nanoparticles at 72 h. To determine whether HGF-loaded nanoparticles could protect the liver when suffering, 10 mg nanoparticles were injected into the blood of C57BL/6 mice 72 hours before the mice were induced acute liver injury and 60 ng and 120 ng HGF solutions were also injected into another two groups for comparison. Besides, a normal mouse group and an untreated model group were also set as a control.

Firstly, HGF levels in the blood and liver tissues were analyzed (Figures 3(e) and 3(f)) using a HGF ELISA kit. The levels of HGF in the blood and liver tissues were higher in mice that were administered either HGF-loaded PLGA nanoparticles or HGF solution when the mice were sacrificed. Compared to the HGF solution groups, the HGF-loaded PLGA nanoparticle-treated groups maintained a higher dose of HGF in the blood and liver tissues. This suggested that our HGF-loaded PLGA nanoparticles could slowly release HGF in the blood and keep HGF at a higher level in the blood and in the liver for a longer period of time.

3.4. HGF-Loaded PLGA Nanoparticles Preserved Liver Morphology and Histology. The liver might lose its luster and become larger because of edema upon the induction of acute liver injury. Livers from HGF-loaded PLGA nanoparticle-treated groups looked closer to normal liver morphology (Figure 3(a)). The liver index can be used to indicate the status of the liver (Figure 3(b)). It was calculated as the liver weight divided by the mouse weight. The liver index indicated that HGF-loaded PLGA nanoparticles improved the liver function under CCl_4-induced acute liver failure.

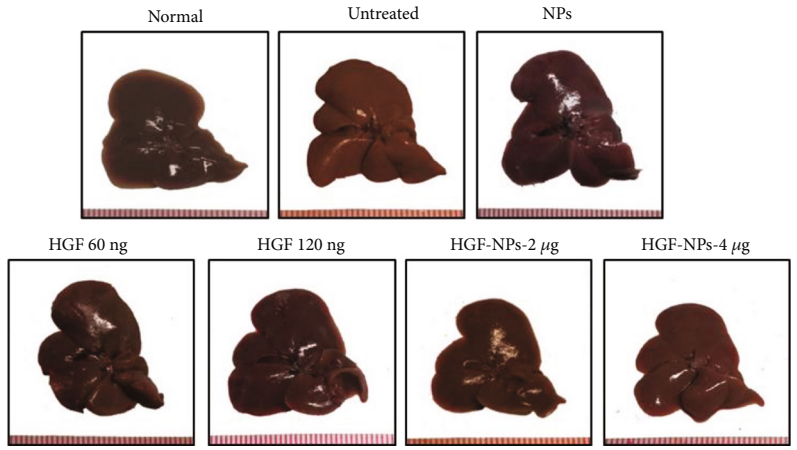

(a)

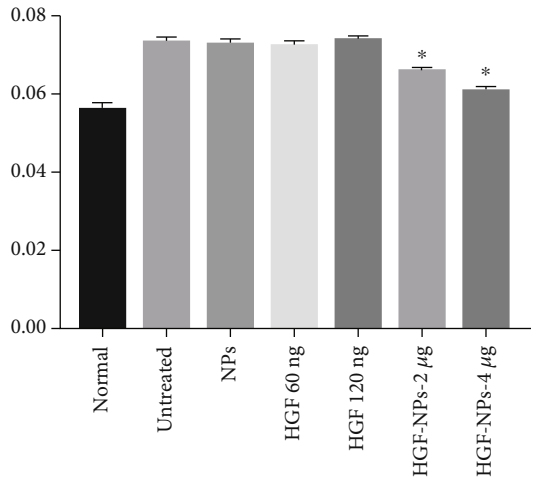

(b)

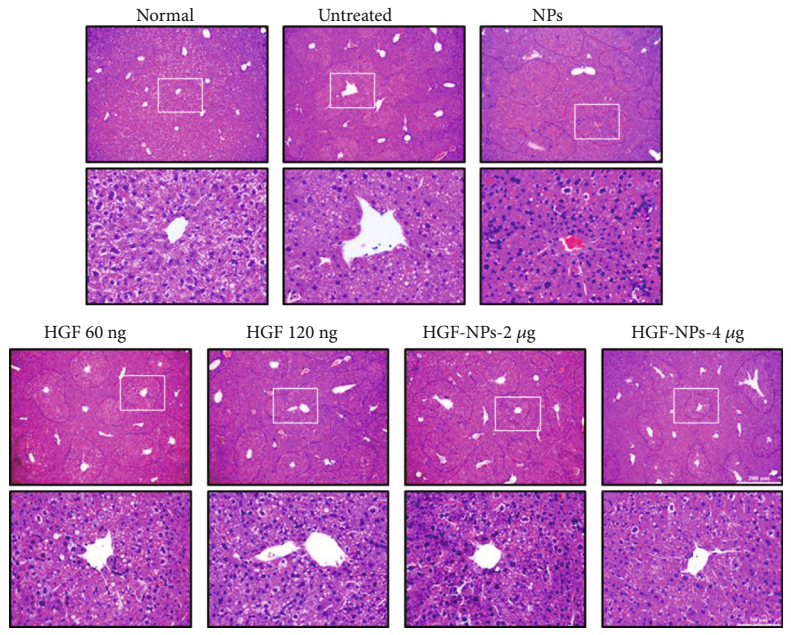

(c)

Figure 3: Continued.

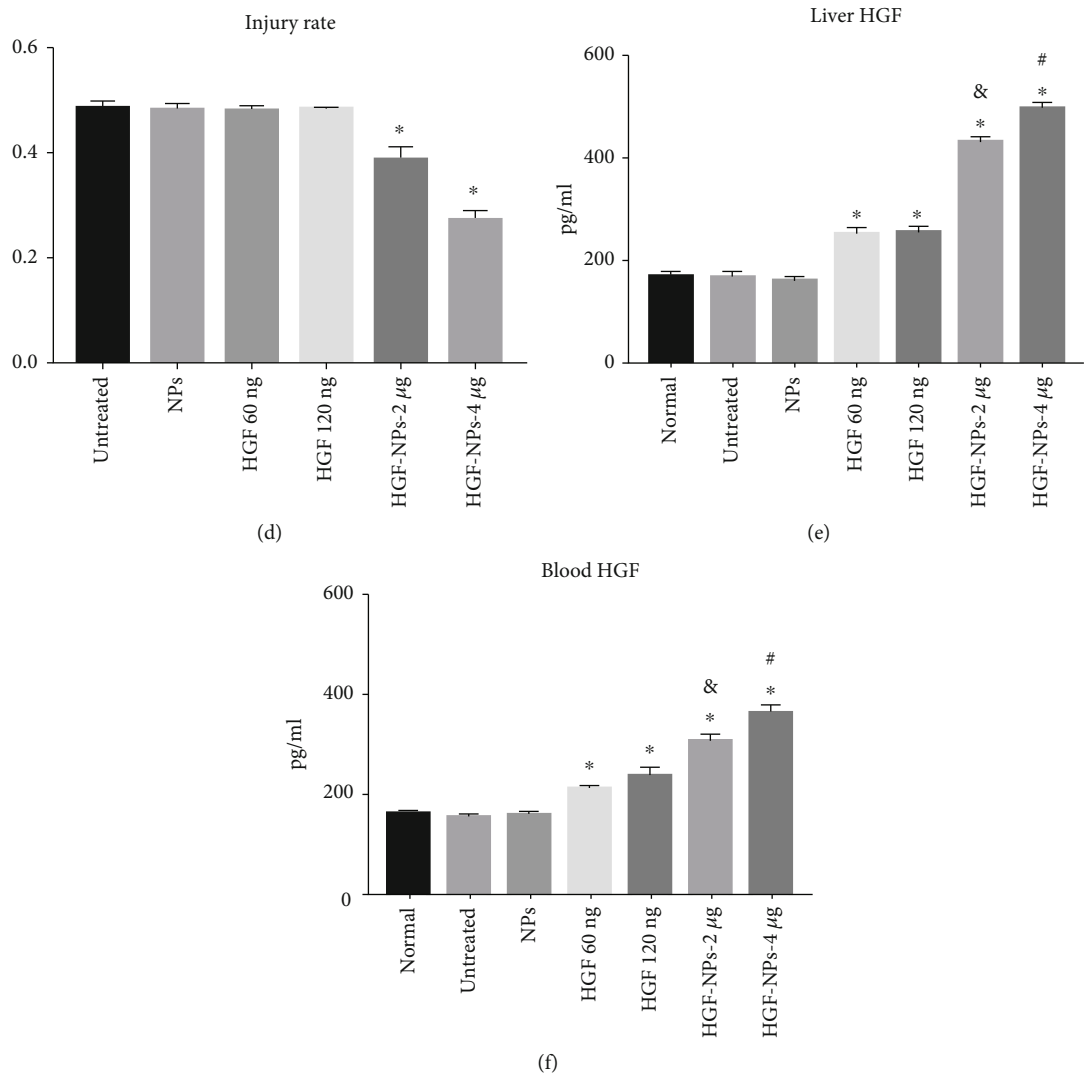

Figure 3: Morphological and histopathological examination of the liver tissue to investigate the influence of HGF-loaded PLGA nanoparticles on acute liver injury induced by CCl_4 in experimental mice. (a) Representative images of the livers of the investigated groups, which included the normal, untreated, NPs, HGF 60 ng, HGF 80 ng, HGF-2 μg-NPs, and HGF-4 μg-NPs groups. The HGF solution groups were injected with a dose of 60 ng HGF or 120 ng HGF through the tail vein to provide the mice an initial concentration of 40 ng HGF per milliliter of blood (40 ng/ml HGF) or 80 ng HGF per milliliter of blood (80 ng/ml HGF), respectively. Approximately 10 mg HGF-2 μg-NPs or HGF-4 μg-NPs was administered into the blood, and they could release 60 or 120 ng HGF, respectively, until the mice were sacrificed. The ruler units are in mm. (b) The liver index of the investigated groups. The liver index was calculated by dividing the liver weight by the mouse weight. $^{*}P < 0.05$ versus the untreated group. (c) Histological analysis of liver sections by hematoxylin and eosin staining. Necrotic areas are encircled with black lines. The pathologic changes of livers from all groups were similar, including necrosis, fatty changes in hepatocytes, and aggregates of inflammatory cells. (d) The injury rate of the tested groups. The injury rate was calculated as the necrotic area divided by the total area under which five fields of the view were analyzed for each group. $^{*}P < 0.05$ versus the untreated group. (e) HGF levels in the blood. (f) HGF levels in the liver homogenate. $^{*}P < 0.05$ versus the normal group, $^{\&}P < 0.05$ versus the HGF 60 ng group, and $^{\#}P < 0.05$ versus the HGF 120 ng group.

Histological analysis of the liver was carried out by H&E staining. The standard morphology of the liver was observed, as shown for the control group (Figure 3(c)). Necrotic areas of hepatocytes were observed in the untreated group. The other groups also showed the same pathologic changes around the centrilobular vein. Necrotic areas of the sections were labeled, and the injury rate was analyzed (Figure 3(d)). HGF-loaded PLGA nanoparticle groups exhibited a slight reduction in hepatocyte death, and the group treated with HGF-NPs-4 μg exhibited decreased inflammation. The HGF solution groups showed no effect on liver morphology or histology, although the HGF levels in the blood and liver tissues were greater than those of the untreated and NP groups.

3.5. HGF-Loaded PLGA Nanoparticles Reduce Liver Damage Markers. To further elucidate the therapeutic effect of HGF-loaded PLGA nanoparticles on liver injury induced by CCl_4,

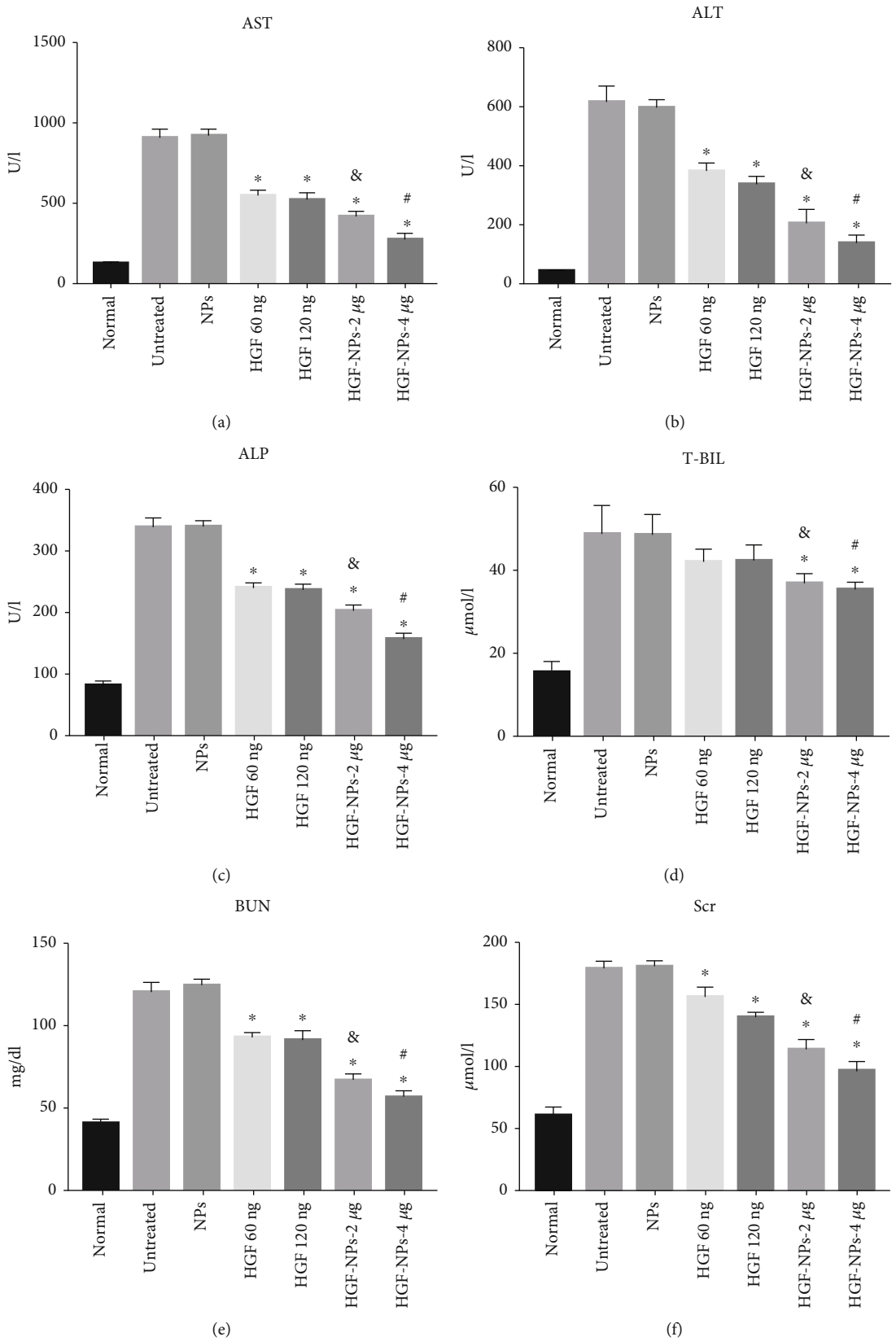

Figure 4: Analysis of serum to investigate the influence of HGF-loaded PLGA nanoparticles on acute liver injury induced by CCl_4 in experimental mice. (a) Aspartate aminotransferase (AST). (b) Alanine aminotransferase (ALT). (c) Alkaline phosphatase (ALP). (d) Total bilirubin (T-BIL). (e) Blood urea N (BUN). (f) Serum creatinine (Scr). The results are presented as the mean ± SD of six mice per group. $^{*}P < 0.05$ versus the untreated group, $^{\&}P < 0.05$ versus the HGF 60 ng group, and $^{\#}P < 0.05$ versus the HGF 120 ng group.

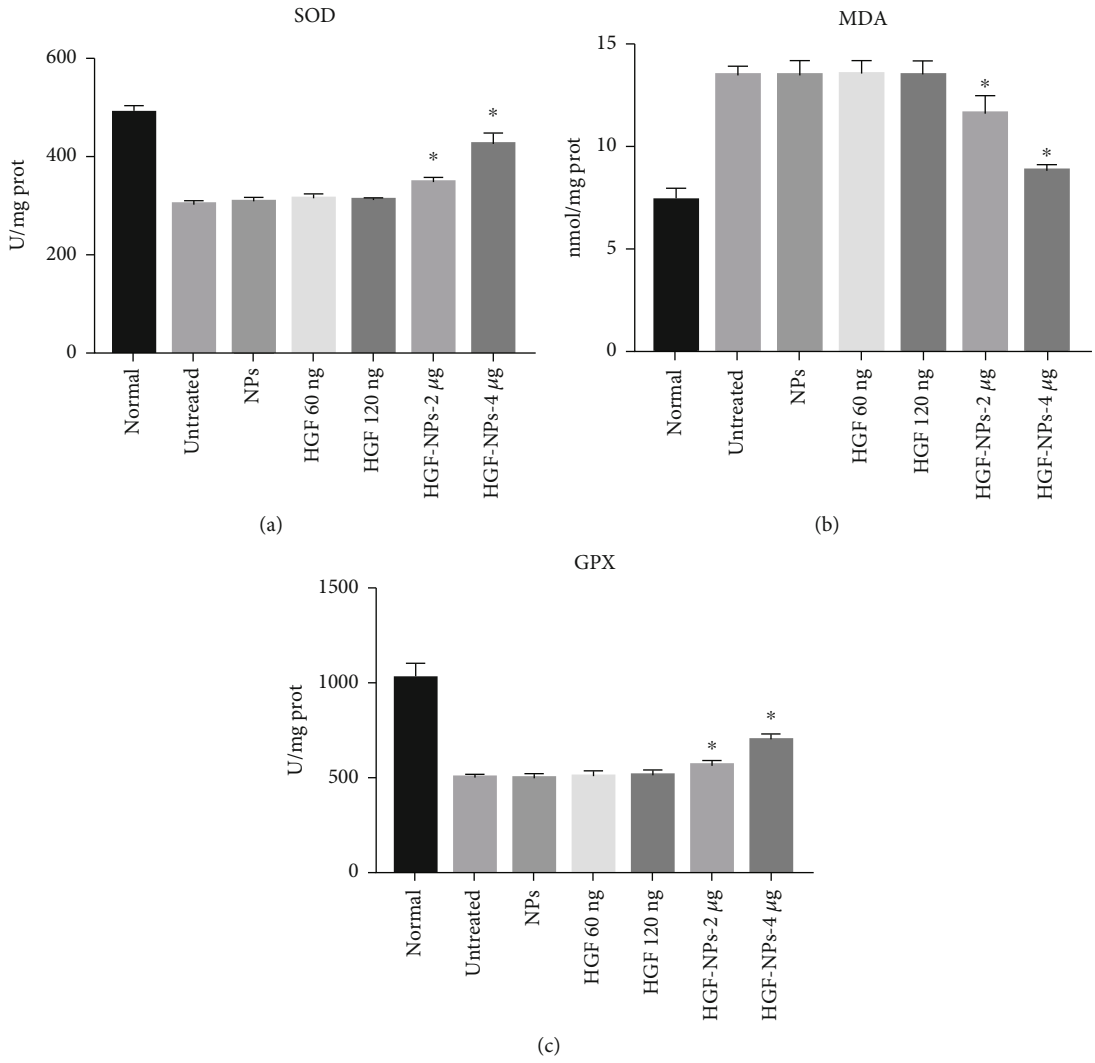

Figure 5: Analysis of the antioxidant index to investigate the influence of HGF-loaded PLGA nanoparticles on acute liver injury induced by CCl_4 in experimental mice. (a) Superoxide dismutase (SOD). (b) Malondialdehyde (MDA). (c) Glutathione peroxidase (GPX). The results are presented as the mean ± SD of six mice per group. $^*P < 0.05$ versus the untreated group.

serum ALT, AST, ALP, and T-BIL were analyzed and are shown (Figures 4(a)–4(d)). The results indicated that the AST, ALT, ALP, and T-BIL levels in serum were much higher in the untreated group compared with the normal group. HGF solution decreased the levels of AST, ALT, and ALP in the CCl_4-induced mice, but T-BIL did not significantly improve. The levels of AST, ALT, ALP, and T-BIL were decreased significantly in the HGF-loaded PLGA nanoparticle groups in a dose-dependent manner. These results indicated that HGF had preventive effects against liver injury caused by CCl_4 treatment and that our HGF-loaded PLGA nanoparticles could provide a more effective treatment.

3.6. HGF-Loaded PLGA Nanoparticles Protect Renal Damage. Since liver and renal functions are closely connected, the renal function markers BUN and Scr were analyzed to evaluate the effect of HGF-loaded PLGA nanoparticles on renal damage from CCl_4. As shown in Figures 4(e) and 4(f), serum BUN and Scr levels after CCl_4 treatment were increased approximately 3 times compared with the normal group, but HGF significantly decreased the BUN and Scr levels. Our HGF-loaded PLGA nanoparticles could reduce the levels even further to protect against renal damage.

3.7. HGF-Loaded PLGA Nanoparticles Improve Liver Antioxidant Ability. To evaluate the effect of our HGF-loaded PLGA nanoparticles on CCl_4-induced liver antioxidant ability, the levels of SOD activity, MDA, and GPX were analyzed (Figures 5(a) and 5(c)). SOD activity and GPX levels in homogenates were significantly decreased, while the MDA level was markedly increased in the untreated group. No significant difference was observed among the untreated group and HGF solution groups. However, the MDA level was significantly reduced in the HGF-loaded PLGA nanoparticle groups, and SOD activity and GPX levels were increased. These results indicate that HGF-loaded PLGA nanoparticles could improve liver antioxidant ability.

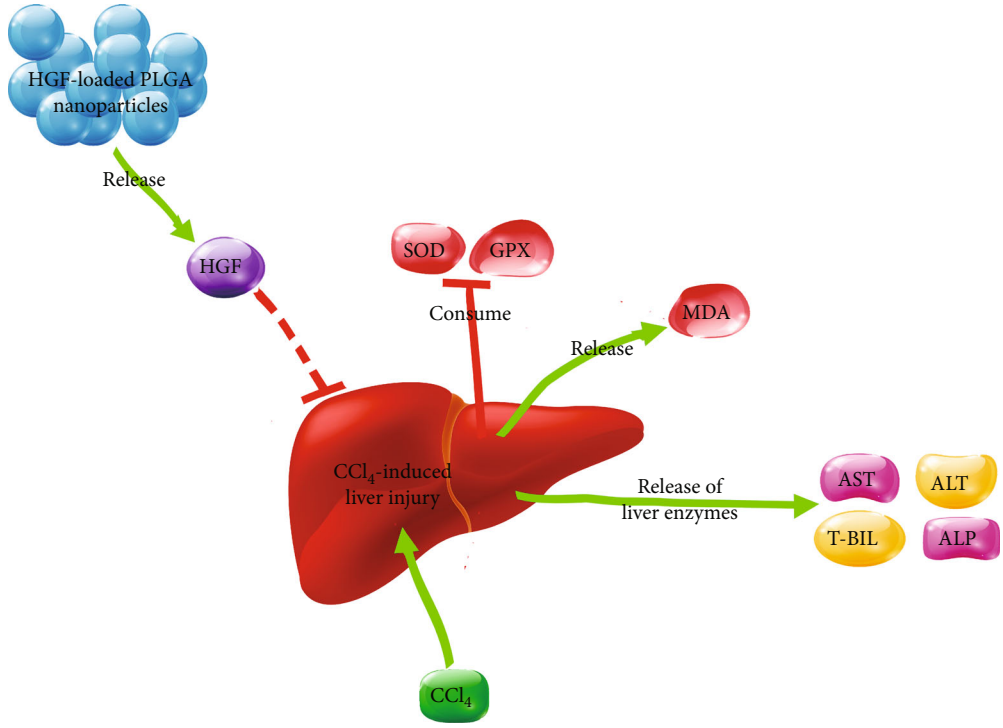

Figure 6: The mechanism of HGF-loaded PLGA nanoparticles on acute liver injury induced by CCl_4 in experimental mice. A single dose of CCl_4 can cause acute liver injury in mice. SOD and GPX are consumed, and MDA is produced and released into blood. In addition, liver enzymes, such as AST, ALT, ALP, and T-BIL, are released into the blood. HGF-loaded nanoparticles may release HGF slowly and maintain HGF at a high concentration. HGF may protect hepatocytes, enhance the antidamage ability of hepatocytes, and protect the vitality of hepatocytes.

4. Discussion

HGF is a growth factor with a variety of biological characteristics and has potential therapeutic effects on various types of liver injury [13, 16]. The effects are generated through the HGF/MET axis [17, 18]. Several studies have confirmed that HGF can promote cell proliferation and migration and inhibit apoptosis and tissue fibrosis [19–21]. Our study suggested that HGF can induce HepG2 cell proliferation in a dose-dependent manner, and at doses of 40 and 80 ng/ml, HGF can significantly promote the proliferation of HepG2 cells.

However, the use of HGF is limited since its half-life is very short (3-5 min). It is unstable in vitro, and it is easily degraded in vivo [13]. To make better use of HGF, a growth factor sustained-release system is needed. Our previous study developed an HGF sustained-release system using PLGA nanoparticles with a good sustained drug release profile and good bioactivity [14]. Since the morphologies and physical characteristics (size, polydispersity, and zeta potential) of the three kinds of nanoparticles were nearly the same as we described in the previous study, it was further indicated in the present study that our process is stable and that our product has good quality.

CCl_4-induced acute liver injury in mice is a widely used model to investigate the prevention and treatment of injury by drugs. CCl_4 is metabolized in the smooth endoplasmic reticulum. It can react with the P450 cytochrome and is decomposed into·CCl_3 and·Cl. CCl_3 covalently binds with membrane lipids and proteins, causing protein metabolism disorders and destruction of the membrane structure and function. In addition, CCl_3 can inhibit the activity of calcium pumps on cell membranes and microsomal membranes. The two pathways eventually result in a series of biochemical changes in the blood [22–24].

In the current study, the protective effects of HGF-loaded PLGA nanoparticles on the CCl_4-induced acute liver injury mouse model were evaluated by the serum ALT, AST, ALP, and T-BIL levels. These enzymes have been widely regarded as important indicators to estimate the severity of acute liver injury since they are released from damaged hepatocytes into the blood [24, 25]. The results showed that our HGF-loaded PLGA nanoparticles could decrease the levels of the four enzymes in the blood in a dose-dependent manner. Our HGF-loaded PLGA nanoparticles were able to slowly release HGF and maintain it at a higher level in the blood and in the liver compared with the HGF solution groups. Although the pathologic changes of livers from all groups were similar, including necrosis, fatty changes in hepatocytes, and aggregates of inflammatory cells, the hepatic necrotic areas were shown to be reduced in the HGF-loaded PLGA nanoparticle groups in a dose-dependent manner. HGF levels in the solution groups were also improved, but the necrotic areas did not improve compared with the untreated groups. We speculated that this might be because the HGF concentrations in the HGF solution groups were not sufficiently high

to cause a marked improvement to hepatic tissues, although the enzyme levels significantly decreased in blood.

In addition, CCl_4 has been reported to induce oxidative injury of the kidney through free radicals ($^{\cdot}CCl_3$) produced by action on the liver [26, 27]. Furthermore, the HGF protein can inhibit tubular cell apoptosis and renal dysfunction and promote the proliferation of cells [8]. In our experiment, serum BUN and Scr were analyzed and showed the same trend as the liver indicator enzymes. Our HGF-loaded PLGA nanoparticles were able to greater inhibit the enzymes than its nonencapsulated form.

Since the main mechanism of CCl_4-induced acute liver injury is lipid peroxidation [24], SOD activity and MDA and GPX levels in the liver were analyzed. SOD is the primary substance that scavenges free radicals in organisms and is the frontline enzyme against free radicals under oxidative stress [28, 29]. MDA is a lipid peroxidation product and is considered an important feature of liver injury [30]. GPX is an important member of antioxidant enzymes [31]. It can effectively eliminate free radicals in CCl_4-induced acute liver injury models. The current study showed that our HGF-loaded PLGA nanoparticles increased SOD activity and GPX levels and decreased MDA levels in the liver compared with the HGF solution groups. These results demonstrated that our HGF-loaded PLGA nanoparticles were more efficient in enhancing the antioxidant capabilities of the liver exposed to CCl_4.

5. Conclusion

HGF is a multifunctional growth factor, but it is unstable and easily degraded. Our study used the W/O/W technique to prepare HGF-loaded PLGA nanoparticles. We demonstrated that our preparation process is stable and that our products are of good quality. This study suggests that HGF-loaded PLGA nanoparticles can provide greater therapeutic benefits for CCl_4-induced acute liver injury, including antilipid peroxidation and a reduction in indicator enzymes of liver injury. These results suggested that the HGF-loaded PLGA nanoparticle sustained-release system may improve the use of HGF and thus promote liver recovery activities (Figure 6).

Data Availability

The data used to support the findings of this study are included within the article.

Conflicts of Interest

The authors declare that they have no conflicts of interest.

Authors' Contributions

Chuxi Lin and Xueer Wang contributed equally to this work.

Acknowledgments

This work is supported by the National Natural Science Foundation of China (81872514, 81600489, and 81703147) and the Natural Science Foundation of Guangdong Province (2014A030312013 and 2017A030310292). The project is also supported by the Science and Technology Planning Project of Guangdong Province (2015B020229002), the Science and Technology Program of Guangzhou (201604020002), and the Chinese Postdoctoral Science Foundation (2018M630966).

Supplementary Materials

Supplementary Table 1: properties of NPs. Physicochemical characterizations of NPs with the 3 measurements from 3 different samples, including size, polydispersity, zeta potential, drug loading, and loading efficiency. Their average and standard deviation (SD) were given. Supplementary Table 2: properties of HGF-NPs-2 μg. Physicochemical characterizations of HGF-NPs-2 μg with the 3 measurements from 3 different samples, including size, polydispersity, zeta potential, drug loading, and loading efficiency. Their average and standard deviation (SD) were given. Supplementary Table 3: properties of HGF-NPs-4 μg. Physicochemical characterizations of HGF-NPs-4 μg with the 3 measurements from 3 different samples, including size, polydispersity, zeta potential, drug loading, and loading efficiency. Their average and standard deviation (SD) were given. Supplementary Figure 1: size of the nanoparticles by intensity. Particle size distribution curves of the three kinds of nanoparticles: red is for NPs, green is for HGF-NPs-2 μg, and blue is for HGF-NPs-4 μg. The nanoparticle sizes were analyzed by a zeta potential analyzer (Zetasizer Nano ZS, Malvern, UK). Supplementary Figure 2: zeta potential of the nanoparticles. Zeta potential distribution curves of the three kinds of nanoparticles: red is for NPs, green is for HGF-NPs-2 μg, and blue is for HGF-NPs-4 μg. The nanoparticle zeta potentials were analyzed by a zeta potential analyzer (Zetasizer Nano ZS, Malvern, UK). *(Supplementary Materials)*

References

[1] S. Sreelatha, P. R. Padma, and M. Umadevi, "Protective effects of *Coriandrum sativum* extracts on carbon tetrachloride-induced hepatotoxicity in rats," *Food and Chemical Toxicology*, vol. 47, no. 4, pp. 702–708, 2009.

[2] E. Shaker, H. Mahmoud, and S. Mnaa, "*Silymarin*, the antioxidant component and *Silybum marianum* extracts prevent liver damage," *Food and Chemical Toxicology*, vol. 48, no. 3, pp. 803–806, 2010.

[3] J. Medina and R. Moreno-Otero, "Pathophysiological basis for antioxidant therapy in chronic liver disease," *Drugs*, vol. 65, no. 17, pp. 2445–2461, 2005.

[4] G. Luo, Y. Shen, L. Yang, A. Lu, and Z. Xiang, "A review of drug-induced liver injury databases," *Archives of Toxicology*, vol. 91, no. 9, pp. 3039–3049, 2017.

[5] H. Yu, L. Zheng, L. Yin et al., "Protective effects of the total saponins from *Dioscorea nipponica* Makino against carbon tetrachloride-induced liver injury in mice through suppression of apoptosis and inflammation," *International Immunopharmacology*, vol. 19, no. 2, pp. 233–244, 2014.

[6] K. Kiso, S. Ueno, M. Fukuda et al., "The role of Kupffer cells in carbon tetrachloride intoxication in mice," *Biological & Pharmaceutical Bulletin*, vol. 35, no. 6, pp. 980–983, 2012.

[7] G. Malaguarnera, E. Cataudella, M. Giordano, G. Nunnari, G. Chisari, and M. Malaguarnera, "Toxic hepatitis in occupational exposure to solvents," *World Journal of Gastroenterology*, vol. 18, no. 22, pp. 2756–2766, 2012.

[8] T. Nakamura, K. Sakai, T. Nakamura, and K. Matsumoto, "Hepatocyte growth factor twenty years on: much more than a growth factor," *Journal of Gastroenterology and Hepatology*, vol. 26, pp. 188–202, 2011.

[9] G. K. Michalopoulos, "Advances in liver regeneration," *Expert Review of Gastroenterology & Hepatology*, vol. 8, no. 8, pp. 897–907, 2014.

[10] A. B. Fajardo-Puerta, M. M. Prado, A. E. Frampton, and L. R. Jiao, "Gene of the month: HGF," *Journal of Clinical Pathology*, vol. 69, no. 7, pp. 575–579, 2016.

[11] A. Valdes-Arzate, A. Luna, L. Bucio et al., "Hepatocyte growth factor protects hepatocytes against oxidative injury induced by ethanol metabolism," *Free Radical Biology & Medicine*, vol. 47, no. 4, pp. 424–430, 2009.

[12] H. Yang, N. Magilnick, M. Xia, and S. C. Lu, "Effects of hepatocyte growth factor on glutathione synthesis, growth, and apoptosis is cell density-dependent," *Experimental Cell Research*, vol. 314, no. 2, pp. 398–412, 2008.

[13] F. Xue, T. Takahara, Y. Yata et al., "Attenuated acute liver injury in mice by naked hepatocyte growth factor gene transfer into skeletal muscle with electroporation," *Gut*, vol. 50, no. 4, pp. 558–562, 2002.

[14] W. J. Xian, X. E. Wang, and L. Zhang, "Construction and bioactivity evaluation of hepatocyte growth factor-loaded poly (lactic-co-glycolic acid) nanoparticles," *Nan Fang Yi Ke Da Xue Xue Bao*, vol. 38, no. 2, pp. 217–223, 2018.

[15] N. M. Lindstrom, D. M. Moore, K. Zimmerman, and S. A. Smith, "Hematologic assessment in pet rats, mice, hamsters, and gerbils: blood sample collection and blood cell identification," *Clinics in Laboratory Medicine*, vol. 35, no. 3, pp. 629–640, 2015.

[16] H. Masunaga, N. Fujise, A. Shiota et al., "Preventive effects of the deleted form of hepatocyte growth factor against various liver injuries," *European Journal of Pharmacology*, vol. 342, no. 2-3, pp. 267–279, 1998.

[17] Y.-W. Zhang, Y. Su, O. V. Volpert, and G. F. Vande Woude, "Hepatocyte growth factor/scatter factor mediates angiogenesis through positive VEGF and negative thrombospondin 1 regulation," *Proceedings of the National Academy of Sciences of the United States of America*, vol. 100, no. 22, pp. 12718–12723, 2003.

[18] Y. Liu, X. Pan, S. Li et al., "Endoplasmic reticulum stress restrains hepatocyte growth factor expression in hepatic stellate cells and rat acute liver failure model," *Chemico-Biological Interactions*, vol. 277, pp. 43–54, 2017.

[19] E. Naguib, A. Kamel, O. Fekry, and G. Abdelfattah, "Comparative study on the effect of low intensity laser and growth factors on stem cells used in experimentally-induced liver fibrosis in mice," *Arab Journal of Gastroenterology*, vol. 18, no. 2, pp. 87–97, 2017.

[20] K. Sakamoto, N. C. Khai, Y. Wang et al., "Heparin-binding epidermal growth factor-like growth factor and hepatocyte growth factor inhibit cholestatic liver injury in mice through different mechanisms," *International Journal of Molecular Medicine*, vol. 38, no. 6, pp. 1673–1682, 2016.

[21] T. Tomiya, M. Omata, H. Imamura, and K. Fujiwara, "Impaired liver regeneration in acute liver failure: the significance of cross-communication of growth associated factors in liver regeneration," *Hepatology Research*, vol. 38, Supplement 1, pp. S29–S33, 2008.

[22] P. Manna, M. Sinha, and P. C. Sil, "Aqueous extract of *Terminalia arjuna* prevents carbon tetrachloride induced hepatic and renal disorders," *BMC Complementary and Alternative Medicine*, vol. 6, no. 1, p. 33, 2006.

[23] J.-Y. Xu, Y. Y. Su, J. S. Cheng et al., "Protective effects of fullerenol on carbon tetrachloride-induced acute hepatotoxicity and nephrotoxicity in rats," *Carbon*, vol. 48, no. 5, pp. 1388–1396, 2010.

[24] P. J. Wills and V. V. Asha, "Protective effect of *Lygodium flexuosum* (L.) Sw. extract against carbon tetrachloride-induced acute liver injury in rats," *Journal of Ethnopharmacology*, vol. 108, no. 3, pp. 320–326, 2006.

[25] B. Lu, Y. Xu, L. Xu et al., "Mechanism investigation of dioscin against CCl4-induced acute liver damage in mice," *Environmental Toxicology and Pharmacology*, vol. 34, no. 2, pp. 127–135, 2012.

[26] S. Uchino, J. A. Kellum, R. Bellomo et al., "Acute renal failure in critically ill patients: a multinational, multicenter study," *JAMA*, vol. 294, no. 7, pp. 813–818, 2005.

[27] S. Raja, K. F. H. N. Ahamed, V. Kumar, K. Mukherjee, A. Bandyopadhyay, and P. K. Mukherjee, "Antioxidant effect of *Cytisus scoparius* against carbon tetrachloride treated liver injury in rats," *Journal of Ethnopharmacology*, vol. 109, no. 1, pp. 41–47, 2007.

[28] C. R. White, T. A. Brock, L. Y. Chang et al., "Superoxide and peroxynitrite in atherosclerosis," *Proceedings of the National Academy of Sciences of the United States of America*, vol. 91, no. 3, pp. 1044–1048, 1994.

[29] C. T. Hsu, "The role of the autonomic nervous system in chemically-induced liver damage and repair - using the essential hypertensive animal model (SHR)," *Journal of the Autonomic Nervous System*, vol. 51, no. 2, pp. 135–142, 1995.

[30] H. H. Draper and M. Hadley, "[43] Malondialdehyde determination as index of lipid peroxidation," *Methods in Enzymology*, vol. 186, pp. 421–431, 1990.

[31] J. Ruszkiewicz and J. Albrecht, "Changes of the thioredoxin system, glutathione peroxidase activity and total antioxidant capacity in rat brain cortex during acute liver failure: modulation by L-histidine," *Neurochemical Research*, vol. 40, no. 2, pp. 293–300, 2015.